A major purpose of the Technical Information Center is to provide the broadest dissemination possible of information contained in DOE's Research and Development Reports to business, industry, the academic community, and federal, state and local governments.

Although portions of this report are not reproducible, it is being made available in microfiche to facilitate the availability of those parts of the document which are legible.

LA-UR-86-4153

Los Alamos National Laboratory is operated by the University of California for the United States Department of Energy under contract W-7405-ENG-36.

LA-UR--86-4153

DE87 003728

TITLE: OPACITY CALCULATIONS FOR LASER PLASMA APPLICATIONS

AUTHOR(S): Norman H. Magee Jr., T-4

MASTER

SUBMITTED TO: Proceedings of Lasers '86 Meeting
November 3-7, 1986
Orlando, FL

DISCLAIMER

Los Alamos National Laboratory
Los Alamos, New Mexico 87545

OPACITY CALCULATIONS FOR LASER PLASMA APPLICATIONS

Norman H. Magee, Jr.
Los Alamos National Laboratory
Group T-4 MS B212
Los Alamos, New Mexico 87545

Abstract

The Los Alamos LTE light element detailed configuration opacity code (LEDCOP) has been revised to provide more accurate absorption coefficients and group means for modern radiation-hydrodynamic codes. The new group means will be especially useful for computing the transport of thermal radiation from laser deposition.

The principal improvement is the inclusion of a complete set of accurate and internally consistent LS term energies and oscillator strengths in both the EOS and absorption coefficients. Selected energies and oscillator strengths were calculated from a Hartree-Fock code, then fitted by a quantum defect method. This allowed transitions at all wavelengths to be treated consistently and accurately instead of being limited to wavelength regions covered by experimental observations or isolated theoretical calculations.

A second improvement is the use of more accurate photoionization cross sections for excited as well as ground state configurations. These cross sections are now more consistent with the bound-bound oscillator strengths, leading to a smooth transition across the continuum limit.

Results will be presented showing the agreement of the LS term energies and oscillator strengths with observed values. The new absorption

Introduction

Our group at Los Alamos National Labortory has been involved in calculating the interaction of radiation with matter for many years. I am here today to report on two improvements we have made in our light element opacity code (LEDCOP), which calculates absorption coefficients and opacities of LTE plasmas for use in the thermal transport of radiation and other plasma applications.

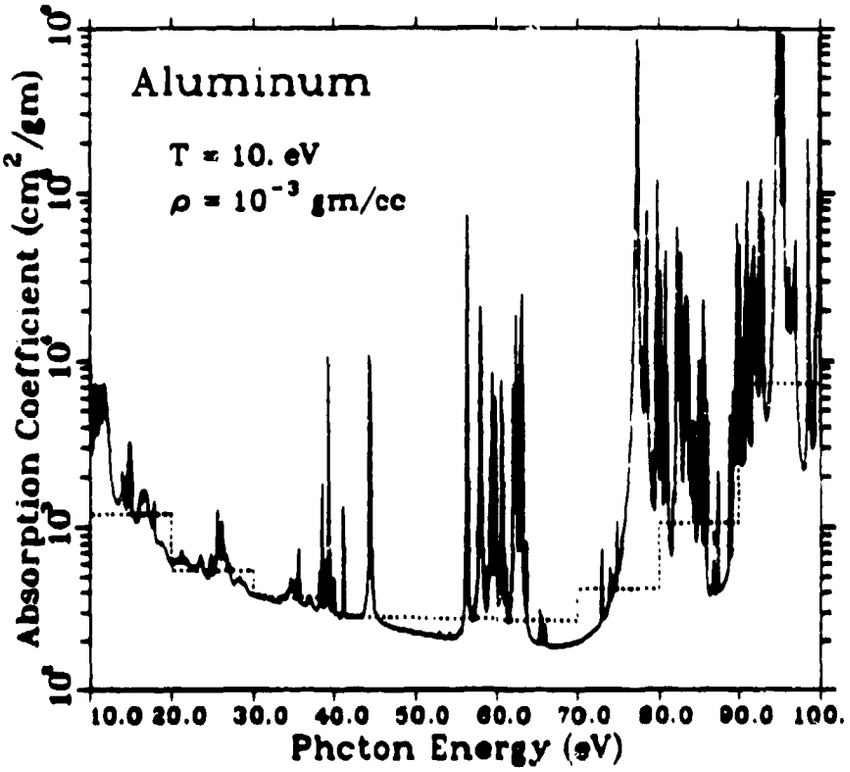

FIGURE 1. Theoretically calculated absorption coefficients for aluminum. The solid curve is the actual calculation and the dashed line represents the group means averaged over 10. eV wide bins.

The solid curve in Figure 1 shows a representative sample of the absorption coefficient output from the code. The absorption coefficient

contains contributions from bound-bound transitions, bound-free photo-ionization, free-free absorption and scattering. The initial use of the code, which dates back over 20 years[1], was to produce Rosseland mean opacities for astrophysical modeling codes. Thus, an integration was preformed over all frequencies to produce a single number (the opacity) for each temperature and density. As computers have become larger and modeling codes more sophisticated, the new generation of radiation hydrodynamics codes have demanded more detailed, frequency dependent information, as might be represented by the dashed line in Figure 1. This curve was produced by taking .0. eV wide energy bins and integrating over the solid curve to produce an average value. One should note that the sample bin structure was not a good choice to represent the solid curve, therefore one really needs to know the major details of the cross sections fairly accurately. We have improved the calculation in two areas. The first area is the bound-bound transitions, where we going to a full LS treatment of the energy levels and the oscillator trengths. The second area is a expansion of the non-hydrogenic bound-free bsorption cross sections to excited edges.

LS Energies and Transitions

Figure 2 shows the line structure for a transition in oxygen IV, assuming hree levels of detail: JJ splitting, LS splitting and configuration veraging. Many codes have only used the single averaged line to represent he transition in their calculations. Our code has used a mixture of he LS transitions and configuration averaged lines, depending on what nformation was available from experiment or theory. Configuration averaged ines really can not be used if one needs detailed frequency dependent nformation. We have decided to go to a full LS treatment, but

plasma. There are two reasons for this. If you use JJ splitting in this simple example, you have 18 lines versus 6 lines for the LS splitting. Even with increased computer capabilities, the JJ splitting is still too much information to handle for all the configurations of all ionization stages of an element. Second, the goal of the code is to calculate group means for radiative transport and not for spectroscopic anaylsis, and the increase in detail is not needed for reasonable width group means.

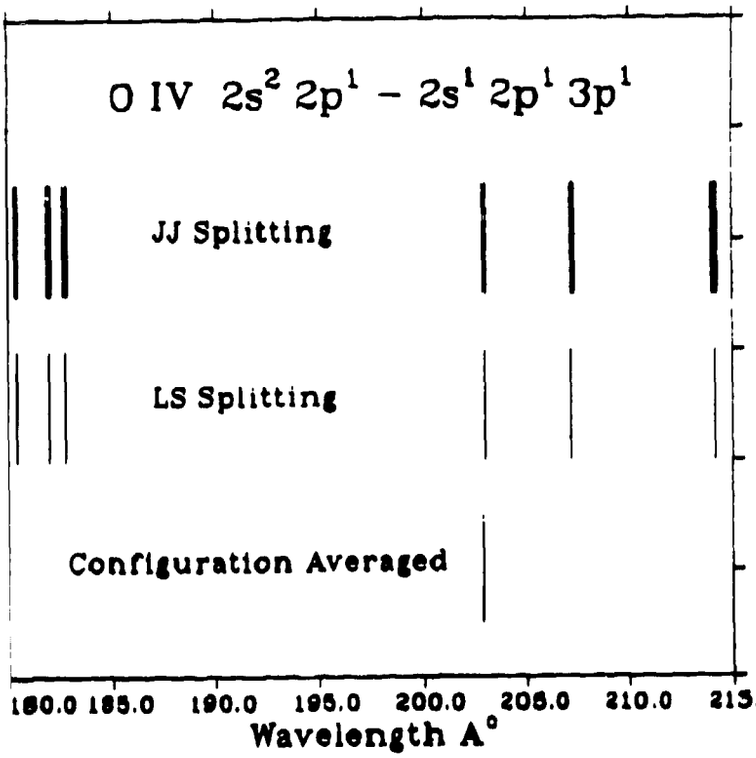

FIGURE 2. Number and wavelength of lines in a 2s - 3p transition of oxygen IV for three different levels of detail

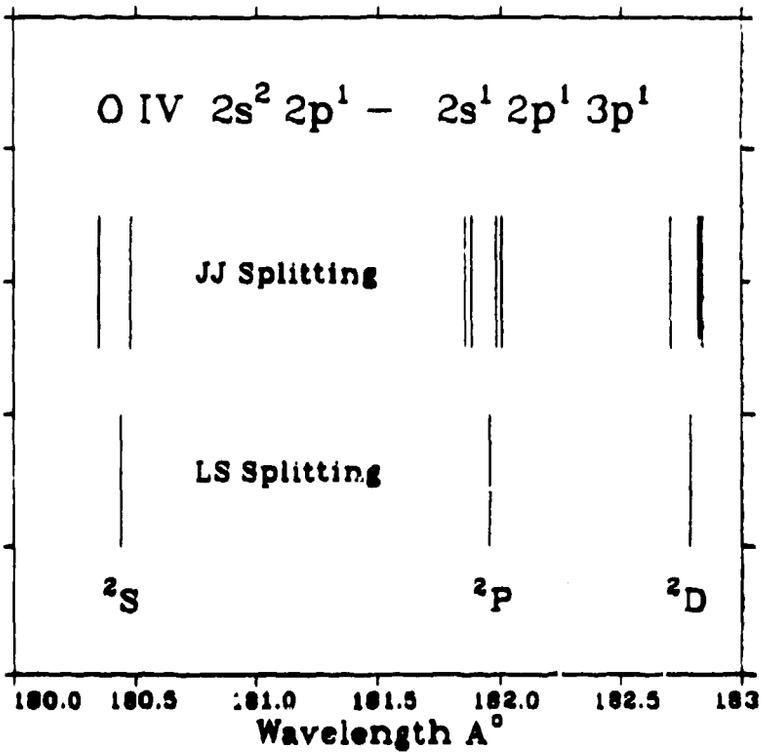

FIGURE 3. The JJ and LS lines of oxygen IV are shown in more detail for three of the LS multiplets.

Figure 3, which shows three multiplets of Figure 2 in more detail, illustrates this point. We are using a Hartree-Fock code of Robert Cowan[2] to calculate the JJ energy levels and oscillator strengths, then averaging to LS

splitting. If you are interested in the deposition of energy at a definite frequency (181.9 A^{o} for example), if you are interested in anaylszing the spectra, you have to retain the full JJ splitting. If you are calculating group means, the fact that you have 3 lines instead of 9 lines will hardly affect the group mean calculation at all, as long as the oscillator strengths are correct and the group mean energy is large compared to the line splitting. The LS spectra should only be used to alert the user that there are lines in the region of his laser frequency. The user should then go to a structures code and find out exact transition energies, oscillator strengths, etc.

We have decided to reduce the amount of stored information even more by fitting the Hartree Fock LS results and storing only the fit coefficients. We use a quantum defect method developed in Los Alamos by Clark and Mertz[3] where the form of the energy fit is shown in equation 1:

$$E = \frac{(Z - N + 1)^2}{(n - (c_0 + c_1/n + c_2/n^2)^2} \quad \text{Ryd.} \qquad (1)$$

where Z = Atomic Z

N = Number of bound electrons

n = Principal shell quantum number.

The linear least square fitting code takes the Hartree-Fock energies (calculated without any configuration interaction or mixing) and fits them to obtain c_0, c_1 and c_2 for a Rydberg series of energies for each S term. The energies are relatively simple to fit and the fit is fast and easy to use. Unfortunately, the oscillator strength fits, which are based on the same Hartree-Fock output, are much more difficult to obtain. The oscillator strength equation is shown below:

$$f = \frac{\text{ANGFAC} * \Delta E * \left|T_{ij}\right|^2}{\quad} \qquad (2)$$

where ANGFAC = Angular scattering factor

ΔE = Transition energy in Rydbergs

$|T_{ij}|$ = Configuration averaged radial dipole matrix element

g_i = statistical weight of the initial multiplet.

ΔE is obtained by using equation 1 to calculate the upper and lower multiplet energies and taking the difference. The angular factors are obtained from Cowan or Condon and Shortley[4] and stored in a data base. Splitting the angular factor out this way is very convienent since it allows one to use a configuration averaged radial dipole matrix element and take full advantage of the angular symmentry to store less data. For instance, if you have the angular factors for neutral oxygen, they are the same for oxygen-like iron, aluminum, etc. Also, the angular terms are the same for similar configurations. A simple example would be: H, Li, B and Na. In transitions involving only the outer electron, all four elements consist of a single electron outside a closed shell and the angular factors are the same for all. This duplication is also true for more complicated configurations and allows one to assemble a relatively small data base for all light elements.

The configuration averaged radial dipole matrix elements $|T_{ij}|$ from the Hartree-Fock code are then fit using the quantum defect formalization. This time there are 6 coefficients, 3 for the initial state and 3 for the final state, and the fit can be highly non linear. However, one ends up with only six coefficients to represent an entire transition array, such as s - p or d - p.

TABLE I. Numerical comparison for oxygen

Calculation	No. Coefficients	No. Output Quantities
Energy Levels	2349	5441
Angular Factors	1467	
Transition Coefficients	768	
Lines		65359
Total	4584	70800

Table I illustrates the advantage in storage requirements if the fits are used instead of the actual numbers. For all ionization stages of oxygen, all principal quantum numbers n up to 10 and all angular momentum values from 0 to 4, it takes 2349 coefficients to produce 5441 LS energy levels. If you add in the angular factors, which will handle all configurations through argon-like, and the coefficients for the transition matrix elements, you obtain over 65 thousand lines. Therefore, less than 5 thousand stored numbers will produce over 70 thousand output numbers. If you have a dilute plasma and the equation of state has to be calculated to n = 50 or 100, you obtain over 150 thousand output numbers for the same number of coefficients.

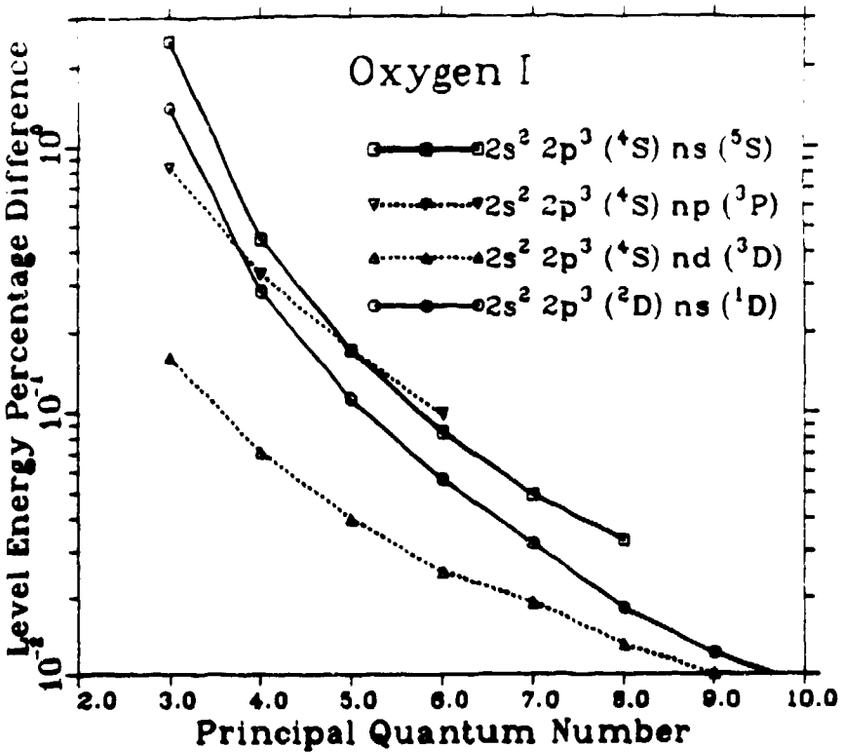

FIGURE 4. Percentage difference between fit energy levels and NBS tables for four Rydberg series of neutral oxygen.

There is, of course, a loss in accuracy in using fits instead of the actual data. Figure 4 shows the percentage difference between the calculated energies and the NBS[5] tables for four rydberg series of neutral oxygen. From a maximum of 2.5 %, the difference drops off to .01 %, the largest errors occuring at the lowest n values as expected. Another point of interest is the trend in the error versus configuration, especially for n = 3. One of the underlying assumptions of the quantum defect method is that the wavefunction of the active electron does not overlap the core. Electrons with lower l values will penetrate the core more and the curves show that the higher l value series are better fit by the quantum defect method. For all ionization stages of oxygen, the maximum error that we have found is 5 %, and this occured where two levels have a strong configuration interaction. Since

our fits are based on Hartree-Fock calculations without configuration mixing, it is not surprising that our largest errors will be where there is strong mixing.

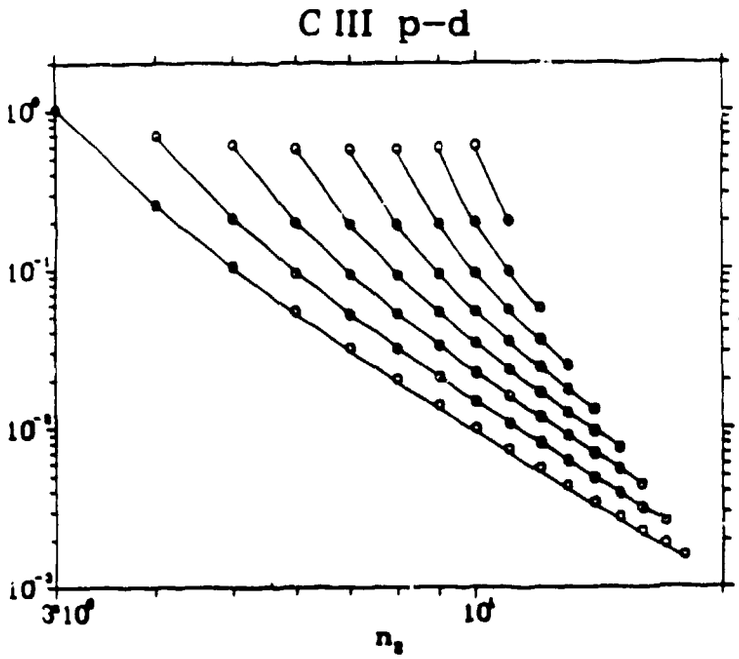

FIGURE 5. Plot of oscillator strength versus final quantum number n' for initial values of n from 2 to 9 for the transition $2s^1\ np^1 - 2s^1\ n'd^1$ in carbon III. The solid lines are the fits and the circles are the initial Hartree-Fock calculated oscillator strengths. This plot printed with permission of Clark and Merts.

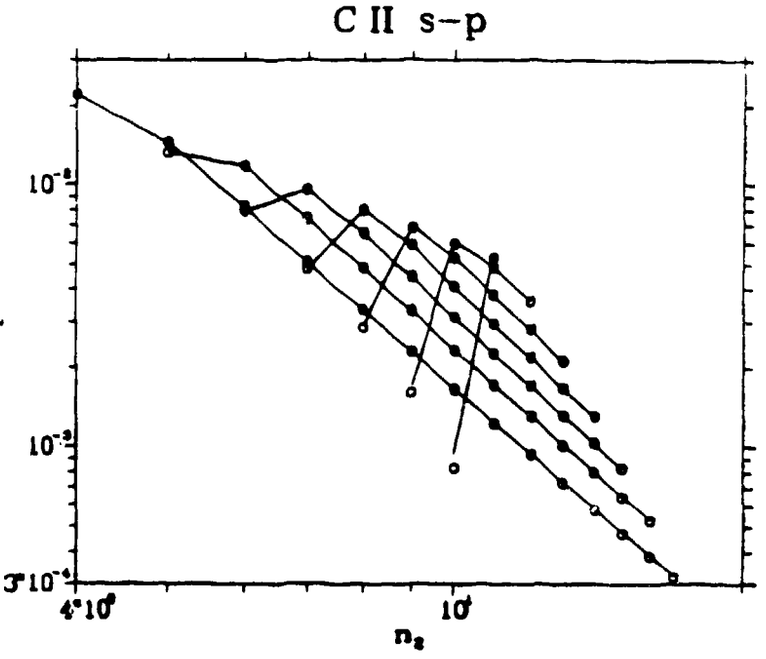

FIGURE 6. Plot of oscillator strength versus final quantum number n' for initial values of n from 3 to 9 for the transition $2s^2\ ns^1 - 2s^2\ n'p^1$ in carbon II. The solid lines are the fits and the circles are the initial Hartree-Fock calculated oscillator strengths. This plot printed with permission of Clark and Merts.

Since it is difficult to obtain a complete series of observed oscillator trengths, we compare the fitted oscillator strengths to the input Hartree- ock numbers. Figures 5 and 6, from the paper by Clark and Merts, show a - d sequence and an s - p sequence. The lowest curve in figure 5 is the 2p nd series, the next curve the 3p to nd series, etc. The maximum error tween the calculated and fit numbers is about 1 %, but this is a relatively sy array to fit. The structure of the array in Figure 6 is much more mplicated as would be expected for an active s electron. Here, the lowest rve is the 3s to np and it has slightly more structure than the p to d rves, but by the time you reach the 6s to np curve, it really bends er. For this oscillator strength array, we have errors on the order of % between the input numbers and the fit. However, when one realizes that e 3s to 4p hydrogenic oscillator strength is .48 and we are getting a number the order of .02, errors of 10 % are relatively negligible compared to the provement from the hydrogenic value. The observed oscillator strength for is transition is .054, but since neutral and near neutral ionization stages ually have strong configuration interaction, which is not included in the rtree-Fock calculations, one should not be surprised at this difference. is does reemphasize the fact that these results are not for spectroscopic alysis, but for group means of reasonalbe energy widths. As long as one nserves oscillator strength and distributes it approximately correctly, the oup means are not going to be seriously affected by errors of this order of gnitude in the weaker oscillator strengths.

Non-Hydrogenic Bound-Free Photoionization

The expansion in use of the non-hydrogenic bound-free cross sections turns out to be just as important as the new bound-bound line treatment. In the past, we have used single configuration, fully relavistic potentials to calculate bound-free cross sections for the levels occupied in the ground state of an atom. For example, neutral aluminum had non-hydrogenic cross sections for the 1s, 2s, 2p, 3s and 3p edges.

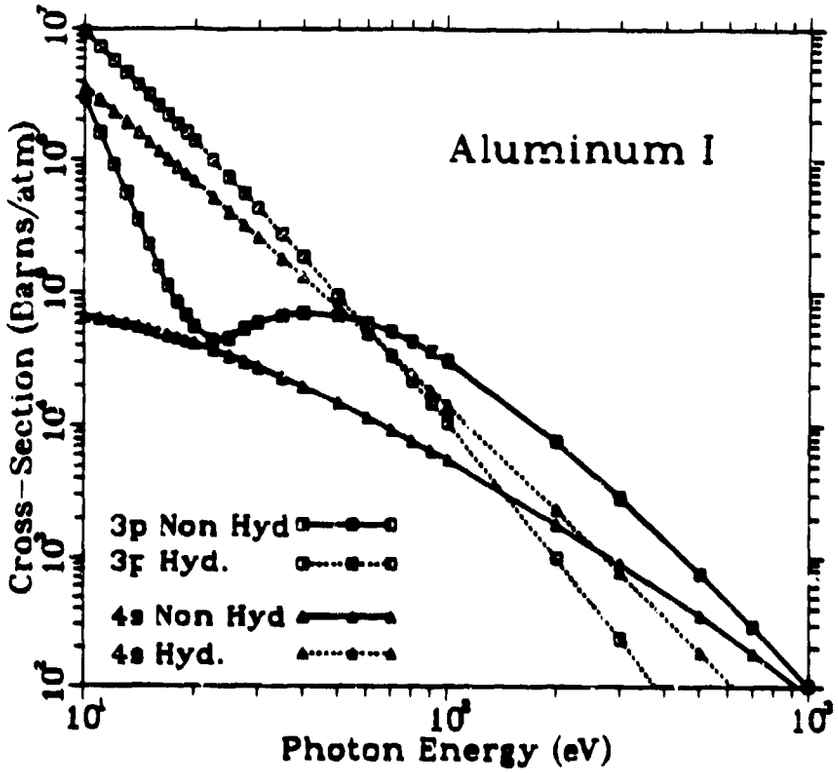

FIGURE 7. Hydrogenic and non-hydrogenic bound-free cross sections of neutral aluminum are plotted for the 3p ground state and the 4s excited state.

Figure 7 shows the difference between the hydrogenic and non hydrogenic 3p cross sections, which can be more than an order of magnitude, as well as having a completely different structure. We have now included non-hydrogenic cross sections for some of the excited edges, such as the 4s

shown in figure 7. These cross sections were not included previously because it was not realized until recently how large the differences were, and it was felt than the occupancies of the excited levels were low enough to ignore the cross section differences. This has turned out not to be the case and in some temperature-density regions, this cross section change is the dominant effect.

Results

Figure 8 illustrates the effect these changes can have on the absorption coefficients. This temperature-density point for aluminum is not typical, but has been picked to show how large the differences can be. Above 10. eV photon energy, the absorption coefficients were dominated by the excited bound-free edges and the hydrogenic $\Delta n \neq 0$ bound-bound transitions. The lower non-hydrogenic bound-free cross sections caused the continuous background to drop by almost an order of magnitude in places. The shift in line strength from above 10. eV to below 10. eV arose from the switch to non-hydrogenic oscillator strengths. Oscillator strength is conserved in both calculations, but the distribution is quite different. Instead of strong $\Delta n = 1,2,$etc. lines and no $\Delta n = 0$ lines, we now have most of the oscillator strength in the $\Delta n = 0$ lines, resulting in the strong lines at 7.5 eV and the disapperence of many lines above 10. eV. Putting both corrections in simultaneously also insures a smooth transition across the continuum limit.

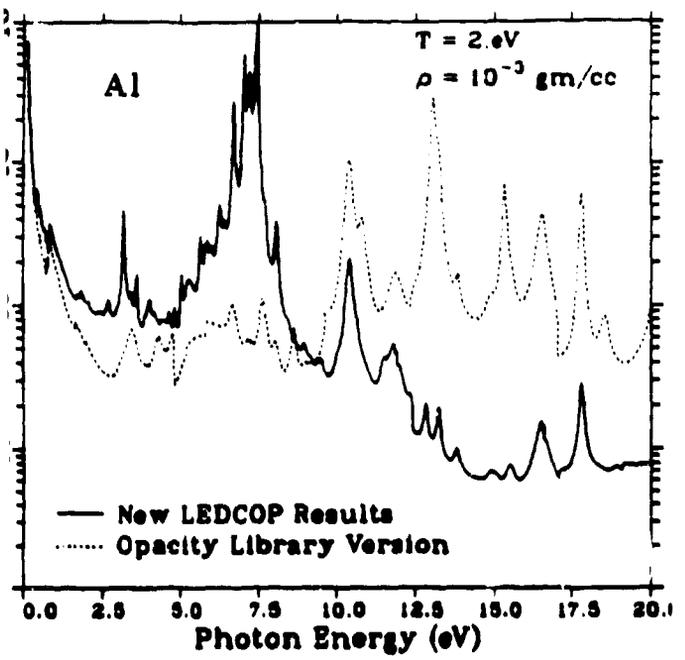

FIGURE 8. Aluminum absorption coefficients illustrating the differences in the bound-bound and bound-free cross sections between the Opacity Library version and the present results.

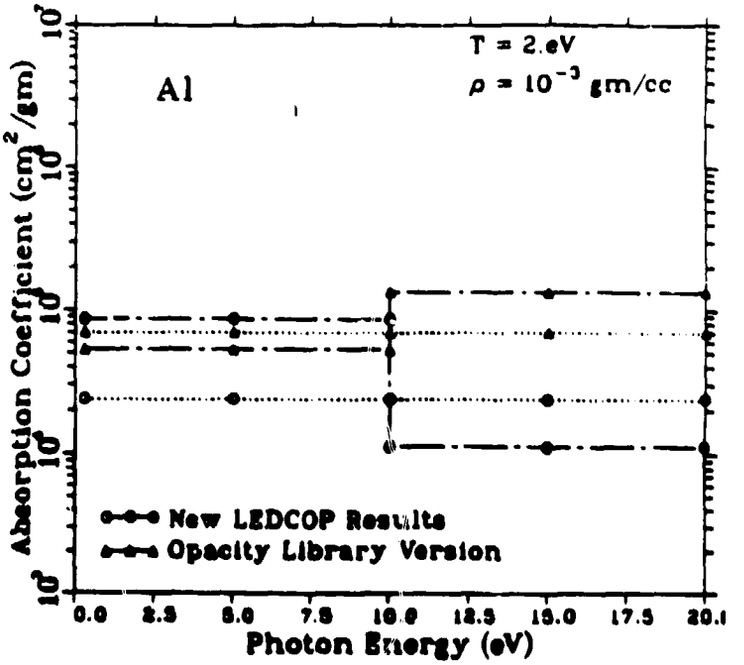

FIGURE 9. Four group mean plots, two for each of the curves in Figure 8, showing the difference in the results, not only for the two data sets but also for the group mean structure.

As has been stated throughout this paper, we are interested in producing tter group means for radiation transport calculations. Figure 9 shows two ts of group means for each curve in figure 8. The two group means over the ll 20. eV photon range differ by a factor of 2 to 3, certainly a significant ange, but not as significant as the changes for the smaller group means from to 10. eV and 10. to 20. eV. Here we have a factor of 2 increase for the st group and an order of magnitude decrease for the second group. This lustrates what we are striving for with this set of changes: more accurate

and detailed group means, where the group mean boundaries are chosen carefully to take into account prominant spectral features, but are not so narrow as to involve one in spectral anaylsis.

References

1. A.N. Cox, Stars and Stellar Systems, Vol. 8, ed. L.H. Aller and D.B. McLaughlin, Chicago: University of Chicago Press (1964).

2. R. D. Cowan, Theory of Atomic Structure and Spectra, Berkeley: University of California Press (1981).

3. R. E. H. Clark and A. L. Merts, "Quantum Defect Method Applied to Oscillator Strengths", (to be published).

4. E. U. Condon and G. H. Shortley, The Theory of Atomic Spectra, University Press Cambridge (1953).

5. C. E. Moore, Selected Tables of Atomic Spectra, NSRDBS-NBS 3 (U. S. Govt. Printing Off., Washington, D. C.) Sec. 7(1976);O I.